

RSC Advances



This is an *Accepted Manuscript*, which has been through the Royal Society of Chemistry peer review process and has been accepted for publication.

Accepted Manuscripts are published online shortly after acceptance, before technical editing, formatting and proof reading. Using this free service, authors can make their results available to the community, in citable form, before we publish the edited article. This *Accepted Manuscript* will be replaced by the edited, formatted and paginated article as soon as this is available.

You can find more information about *Accepted Manuscripts* in the [Information for Authors](#).

Please note that technical editing may introduce minor changes to the text and/or graphics, which may alter content. The journal's standard [Terms & Conditions](#) and the [Ethical guidelines](#) still apply. In no event shall the Royal Society of Chemistry be held responsible for any errors or omissions in this *Accepted Manuscript* or any consequences arising from the use of any information it contains.

ARTICLE

Ultrahigh molecular weight lignosulfonate-based polymers: preparation, self-assembly behaviours and dispersion property in coal-water slurry

Cite this: DOI: 10.1039/x0xx00000x

Received 00th XXX XXX,
Accepted 00th XXX XXX

DOI: 10.1039/x0xx00000x

www.rsc.org/

Nanlong Hong^{a,b}, Yuan Li^{a,b*}, Weimei Zeng^{a,b}, Mengke Zhang^{a,b}, Xinwen Peng^{b*}, and Xueqing Qiu^{a,b*}

Abstract: Using a novel and facile method, we report a family of ultrahigh molecular weight lignosulfonate-based polymers (ALSs) via alky chain coupling polymerization. Gel permeation chromatography (GPC) showed a significant increase in weight-average molecular weights (Mws) from 42800 Da of ALS1 to 251000 Da of ALS5 as one of the highest Mws among reported lignosulfonates (LSs), to date. Functional group content measurements, FTIR and ¹H-NMR confirmed the efficient polymerization by nucleophilic substitution coupling mechanism and suggested a straightforward relationship between the polymerization of lignosulfonate (LS) and consumption of phenolic hydroxyl groups. Moreover, hollow nanospheres were obtained via self-assembly of water soluble ALS and investigated by DLS, SEM, TEM and AFM. The hollow sphere structure with a hydrophilic core and a hydrophobic shell was confirmed by XPS and elemental analysis. Stable quasi-solid nanospheres were obtained from ALS by the addition of cetyl trimethyl ammonium bromide (CTAB). Furthermore, ALS2 with relatively high molecular weight showed unexpected better dispersion properties than raw material LS and naphthalene sulfonate formaldehyde condensate (NSF) for coal-water slurry. The effective polymerization route to improve Mw and the self-assemblies from polymer-only ALS provided novel avenues for high value application of lignin, a sustainable and abundant bioresource.

Introduction

Polymer nano- and micro- materials have been a growing research field over decades of years as they showed potential application as multi-function materials in various nanosciences and technologies.¹⁻⁵ Generally, synthetic amphiphilic block or graft copolymers have been extensively studied to prepare nano-/micro- structures via several methods including template synthesis,^{6,7} self-assembly,⁸ emulsion polymerization,^{9,10} and core removal of dendrimers.¹¹ It is well known that biocompatibility and biodegradability are required for the design of polymer. It will be a promising approach that we can readily obtain water soluble polymer from bioresource, such as lignin or lignosulfonate (LS). Recently, based on previous studies on the self-assembly of lignin and LS to obtain colloidal spheres from our research group,^{12,13} we found that alky chain coupling lignosulfonate-based polymer (ALS), an amphiphilic biopolymer obtained from alky chain coupling polymerization of lignosulfonate, can directly and readily produce polymer nanospheres in selective solvent via self-assembly without any templates. This result has been rarely reported previously.

With the increasing concern on the fossil energy and environment pollution problems, it is extremely important to

address them by the efficient utilization of abundant and renewable bioresource including cellulose¹⁴⁻¹⁶ and lignin¹⁷⁻¹⁹ etc. Lignin, the second most abundant renewable bioresource material, has stimulated great fundamental interest for widespread applications in industrial technology for a long time. Molecular weight is one of the critical factors that determine the properties of dispersant based on lignosulfonate. For example, LSs with relatively high Mws exhibited positive effects on viscosity-reducing properties of coal-water slurry (CWS).^{20,21} High Mw accompanied with large steric hindrance plays as a key role in dispersion properties on TiO₂ suspension.²² Moreover, LSs with high Mws also exhibit good performances as dispersants for dimethomorph water-dispersible granule (DWG)²³ and water reducing agents for cement-water systems.²⁴ In addition, the exploitation of such a biocompatible and biodegradable material to prepare nanomaterials is of crucial importance for the development of novel and high value-added application.²⁵⁻²⁷

In order to fabricate nanomaterials with LS polymer, LS should be modified to adjust its hydrophobic property and increase Mw. The alky chain coupling polymerization of LS could be treated as a hydrophobic modification to obtain

suitable amphiphilic property of LS for the self-assembly behaviour, which was rarely reported, to date. Numerous studies have been focused on the modification of LS by various technologies to increase Mw in order to facilitate its application value in industrial fields. To our knowledge, the main technologies including formaldehyde condensation polymerization,²⁸ graft copolymerization,²⁹ graft sulfonation,³⁰ and enzyme catalysis reaction³¹ were used to improve Mws. Compared with the previous modification routes, our method is easy processing and highly efficient procedure. It is expected to improve the Mw of LS with low Mw from industrial processes such as SPORL (Sulfite Pretreatment to Overcome Recalcitrance of Lignocelluloses) reported by Zhou and co-workers³².

In this paper, ultrahigh Mw linosulfonate-based polymer ALSs were prepared and used as amphiphilic biopolymer to prepare hollow nanospheres via self-assembly. The formation mechanism of hollow spheres was investigated by dynamic light scattering (DLS), scanning electron microscopy (SEM), transmission electron microscopy (TEM), atomic force microscopy (AFM) and X-ray photoelectron spectroscopy (XPS). Furthermore, stable quasi-solid nanosphere obtained from the complex between ALS and cetyl trimethyl ammonium bromide (CTAB) was also detected by TEM, AFM, elemental analysis and XPS. Thus it makes ALS polymer potentially useful in new applications due to the presence of electrostatic attraction between sulfonic groups and guest molecules with cationic groups. Moreover, ALSs exhibited unexpected better dispersion properties than naphthalene sulfonate formaldehyde condensate (NSF) in coal-water slurry.

Experimental section

Materials

LS was supplied by the Quanlin paper mill (Shandong province, China). 1,6-dibromohexane ($C_6H_{12}Br_2$) was supplied by Energy Chemical Co. Ltd. (Shanghai, China) with a purity of 97%. All other chemicals were of analytical grade, including sodium hydroxide (NaOH), potassium iodide (KI), hexane, ethanol (EtOH) and cetyl trimethyl ammonium bromide (CTAB). NSF, naphthalene sulfonate-formaldehyde condensate (commercially available high performance dispersant from Zhanjiang additive company, Guangdong, China) was tested for comparison with ALSs.

Shenhua coal (Shenfu, Shanxi, China) was used to prepare coal-water slurry. Before the preparation of coal-water slurry, raw coal was comminuted with the ball mill to obtain coal powder. Then the coal powder was screened through a 100-mesh screener (0.150 mm pore size) and 70-mesh screener (0.212 mm pore size) to obtain bimodal distribution products with an average particle size of 30 μm .

Preparation of ALSs

LS (10 g) were dissolved in 50 mL of H_2O and NaOH was used to adjust the pH value of the aqueous solution to 11, then the reaction liquid was added different proportions of $C_6H_{12}Br_2$ and trace amount of KI (0.1 g) at 70 $^{\circ}\text{C}$, respectively. The polymerization was stopped after reflux at 70 $^{\circ}\text{C}$ for 8 hours. The synthetic approach was shown in Scheme S1 in Supporting Information. The samples were then extracted with hexane to remove the excessive $C_6H_{12}Br_2$ and the polymers in aqueous solution were filtered. The filtrates were diluted to 0.15 g mL^{-1} and desalted by ion-exchange resin. The purified products were then freeze-dried to obtain yellow brown solid powder samples. The ratios of m (LS):m ($C_6H_{12}Br_2$) were 1:0.08, 1:0.12, 1:0.16, 1:0.24 and 1:0.30, which were named as ALS1, ALS2, ALS3, ALS4 and ALS5, respectively. The proposed structure of the ALS polymer is shown in Figure 1.

Preparation of hollow nanospheres with ALS

ALS polymer was first dissolved in water to prepare 0.5 mg mL^{-1} ALS aqueous solution, followed by the addition of ethanol to achieve the solution of 0.05 mg mL^{-1} . Then, the mixed solution was stirred for 3 h and left for 1 h at room temperature to obtain the ALS hollow nanospheres.

Preparation of quasi-solid nanospheres with ALS and CTAB

ALS polymer was first dissolved in water to prepare 0.5 mg mL^{-1} ALS aqueous solution. CTAB dissolved in ethanol was added into the above ALS aqueous solution (CTAB/ SO_3H =1.5/1, n/n) to achieve a solution of 0.05 mg mL^{-1} . Then, the mixed solution was stirred for 3 h and left for 1 h at room temperature to obtain the quasi-solid nanospheres with ALS and CTAB.

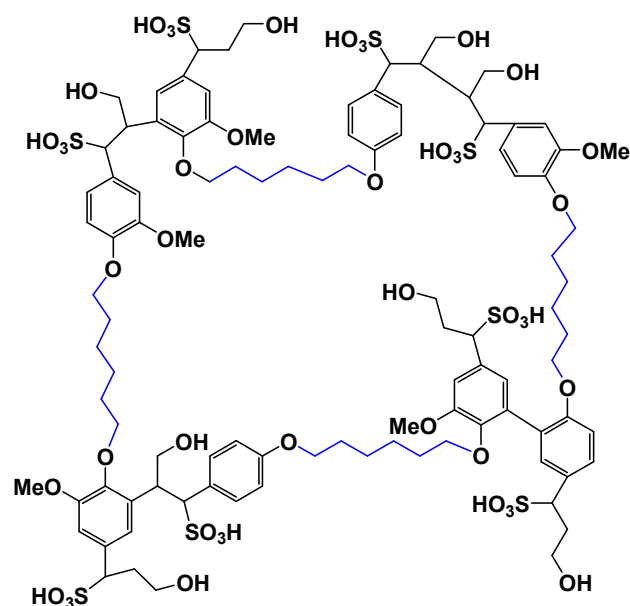


Fig. 1 The proposed structure of the ALS polymer

Characterization

The Mw measurement was conducted by aqueous gel permeation chromatography and the UV absorption at 280 nm was monitored with a Waters 2487 UV detector (Waters Co, Milford, MA, USA). Polystyrene sulfonate was used as calibration standard. A 0.10 M NaNO₃ solution (pH 8.0) was used as mobile phase (0.50 mL min⁻¹). All samples were dissolved and diluted into 0.3 wt% using double-distilled water and filtered by a 0.22 μm filter.

The phenolic hydroxyl group (-OH) content of samples was determined by Folin-Ciocalteu colorimetric (FC) method.³¹ The sulfonic group (-SO₃H) content of LS and ALSs was measured by automatic potentiometric titrator (Type 809 Titrand, Metrohm Corp., Switzerland).³³

Fourier transform infrared spectrometry (FTIR) of Auto system XL/I-series/Spectrum2000 (Thermo Nicolet Co., Madison, WI, USA) was used for infrared spectrum analysis and recorded between 4000 and 400 cm⁻¹. The measurement method was potassium bromide pressed-disk technique. The ¹H-NMR spectra of samples were recorded with 30 mg of each sample dissolved in 0.5 mL of deuterium oxide (D₂O) using DRX-400 spectrometer (Bruker Co., Ettlingen, Germany).

Scanning electron micrographs were recorded with a Nova Nano SEM instrument (Zeiss, Netherlands). Samples were mounted on aluminum stubs by means of double-sided conductive adhesive and sputtered with Au/Pd to reduce charging effects.

TEM images were obtained using a HITACHI H-7650 electron microscope with an accelerating voltage of 200 kV. The TEM samples were prepared by dropping diluted sample solution onto the copper grids coated with a thin carbon film.

Dynamic light scattering (DLS) experiments were performed on Zeta PALS instrument (Brookhaver, America). The concentration of samples was 0.05 mg mL⁻¹ in Ethanol/H₂O (v/v, 9:1) at around pH 7.0.

Atomic force microscopy (AFM) was employed to observe the morphology of hollow and quasi-solid spheres after carbonation. AFM images were recorded using Park XE-100 instrument by tapping mode. The hollow and quasi-solid spheres on the silicon wafer were charred in a tube furnace under nitrogen (N₂) atmosphere. The temperature increased from 25 °C to 800 °C with a heating rate of 5 °C/min. The carbonation process was held at 800 °C for 2.0 h. Then the samples were cooled to room temperature naturally and AFM was conducted to observe the morphology of their residues after pyrolysis.

Elemental analyses were measured by Elementar Vario EL cube. Elemental distribution on the surface of ALS hollow nanospheres was also analyzed by X-ray photoelectron spectroscopy (XPS, Utra Axis DLD, Kratos, England). The elemental distribution of quasi-solid nanospheres obtained with the aggregates of the complex between ALS and CTAB via self-assembly was also detected by elemental analysis and XPS method.

Viscosity measurement of coal-water slurry with LS, ALSs and NSF dispersants was performed employing a rheometer (Haake MARS III). The shear rate range is up run with range of

0–200 s⁻¹ and the temperature is kept at 25 °C, with a fluctuation of 1 °C. The dosage of dispersant is 0.6 wt.%, and the coal content of CWS is fixed at 60 wt.%. The coal powder was slowly mixed in a pot adding a fixed amount of dispersant and water. The slurry was stirred for 10 min at 1200 rpm to disperse the coal particles uniformly in CWS, and the apparent viscosity of the slurry was measured by rheometer. Table S1 shows the results of the proximate and ultimate analyses for Shenhua coal. The Shenhua coal powder has high inherent moisture (M_{ad}) and O/C ratio, which suggest that it is a kind of low rank coal and difficult to prepare CWS with high coal content such as 60 wt.% even for a commercially used dispersant NSF with excellent properties in industry.

Results and discussions

Characterization of ALSs

As shown in Figure 2a, the influence of C₆H₁₂Br₂ on the molecular weight of ALSs was apparent. Mw increased gradually with increasing the proportion of C₆H₁₂Br₂. The results of Mw distribution were listed in Table 1. As shown in Table 1, when LSs were coupled with different amounts of C₆H₁₂Br₂, the LSs underwent more extensive polymerization.

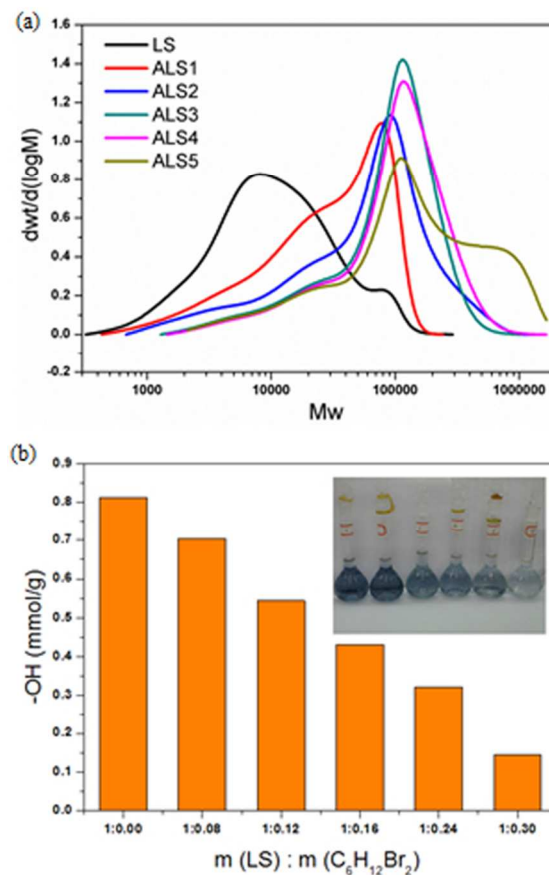


Fig. 2 (a) Effect of 1,6-dibromohexane on Mw distributions of ALSs. (b) Effect of 1,6-dibromohexane on phenolic hydroxyl group contents of ALSs (photos inserted from Left to right: LS, ALS1, ALS2, ALS3, ALS4, ALS5 solution samples after the addition of FC reagent).

With *m* (LS): *m* (C₆H₁₂Br₂) of 1:0.30, the *M_w* of ALS achieved the maximum value by a factor of more than 20-fold of LS. With different proportion of *m* (LS): *m* (C₆H₁₂Br₂), ALS products with different *M_w*s could be easily obtained shown in Table 1. The polydispersity indexes (PDIs) were also listed in Table 1, PDI of ALS5 was the highest among the samples, which was generated by the parts of higher molecular weights. However, from the viewpoint of environmental protection, 1,6-dibromohexane is also toxic, meanwhile, new and green reagent should be developed in future work.

In order to study the influence of C₆H₁₂Br₂ on the structure of LSs, functional groups, such as phenolic hydroxyl groups and sulfonic groups, were investigated. As shown in Figure 2b, obviously, with different proportion of C₆H₁₂Br₂, *M_w*s of ALSs increased accompanied by a decrease of phenolic hydroxyl group contents remarkably. The results were listed in Table 1, phenolic hydroxyl group content of ALS5 with highest molecular weight was just 0.15 mmol g⁻¹. This suggested a straightforward relationship between the polymerization of LS and consumption of phenolic hydroxyl groups.

Table 1 Effect of 1,6-dibromohexane on the molecular weight distributions and functional group contents of ALSs.

Sample	<i>m</i> (LS): <i>m</i> (C ₆ H ₁₂ Br ₂)	<i>M_w</i> /Da	<i>M_n</i> /Da	PDI	-SO ₃ H (mmol g ⁻¹)	-OH (mmol g ⁻¹)
LS	1:0.00	13100	3350	3.91	1.82	0.81
ALS1	1:0.08	42800	11200	3.82	1.31	0.71
ALS2	1:0.12	95400	21300	4.48	1.21	0.54
ALS3	1:0.16	115000	33700	3.41	1.16	0.43
ALS4	1:0.24	135000	38100	3.54	1.03	0.32
ALS5	1:0.30	251000	45200	5.55	1.01	0.15

The sulfonic group contents were also detected and analysed showed in Table 1. With the increase of proportion of *m* (LS): *m* (C₆H₁₂Br₂), sulfonic group contents decreased slightly from 1.82 to 1.01 mmol g⁻¹. The results could be explained by the increase of *M_w* due to the increasing introduction amount of alkyl chains. The alky chain coupling polymerization with C₆H₁₂Br₂ to improve *M_w* of LS could change the amphiphilic property by increasing the hydrophobicity, however, the total amount of sulfonic group could be unchanged by alky chain coupling polymerization, thus the sulfonic group contents (mmol g⁻¹) decreased slightly with the increase of *M_w*.

The detailed water solubility of ALS was tested carefully in current study. The solubility of ALS with *M_w* less than 80 kDa is about 200 mg mL⁻¹, but that of ALS with *M_w* more than 100 kDa decreased to 60 mg mL⁻¹. As is known to us, low dosage of dispersant was usually required for many applications including coal-water slurry, pesticide suspension concentrate and cement-water suspensions, as mentioned in previous introduction²⁰⁻²⁴. Therefore, ALS can meet the requirement basically in industrial applications.

In order to further investigate the influence of C₆H₁₂Br₂ on the chemical structure of raw material LS, the FTIR spectra of LS and ALSs was measured, as shown in Figure 3a. The areas

of bands at 2938 cm⁻¹ and 2864 cm⁻¹ corresponded to methylene stretching vibrations from alkyl chain.³⁴ The areas at 1141 cm⁻¹ corresponded to a combination of C-O bond stretching vibrations.³⁵ As shown in Figure 2a, the adsorption intensities of -CH₂/CH₃- and C-O in ALSs were both increased compared to LS as a result of efficient substitutions of aliphatic chains on phenolic groups of LS. In addition, S-O bonds (band at 1038 cm⁻¹ and 653 cm⁻¹)²¹ were all observed in LS and ALSs, but the adsorption intensities of ALSs were decreased slightly compared to the raw feedstock LS, which was in good agreement with the results of sulfonic group contents measurement. Moreover, the adsorption intensities of aromatic ring stretching vibrations (bands at 1512 cm⁻¹ and 1601 cm⁻¹)³⁴ were all detected in LS and ALSs and exhibited no observable change between raw material and ALSs, which suggested that the aromatic ring structure of LS molecules has not destroyed in the process of reaction.

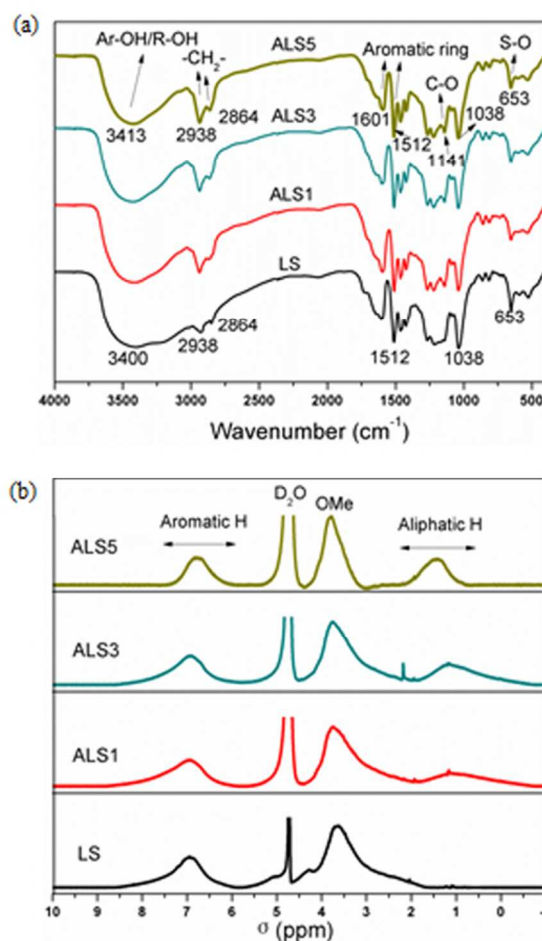


Fig. 3 Spectroscopic analyses of SL and ALSs: (a) IR spectra, (b) ¹H-NMR spectra.

As shown in Figure 2b, the ¹H-NMR spectra of LS and ALSs with quantitative samples were also investigated to further study the change of chemical structure in LS. The ¹H-NMR spectra were obtained from 30mg samples dissolved in 0.5 mL D₂O. The signals between 0.5 and 2.0 ppm were associated

with aliphatic chain.^{36,37} The signal intensity of aliphatic protons exhibited significant increase with the increase of Mws of ALSs, which was in good agreement with the FTIR results. The dramatic increase of aliphatic proton signals came from the efficient coupling of $-C_6H_{12}-$ groups. In addition, it is worth mentioning that the signal intensity of methoxyl protons at 4.00-3.70 ppm exhibited no observable change between LS and ALSs, which means that the alky chain coupling polymerization did not destroyed the methoxyl group.

The results of GPC, functional group content measurements, FTIR, 1H -NMR demonstrated that the effective intermolecular nucleophilic substitution reactions between $C_6H_{12}Br_2$ and LS molecules simultaneously occurred efficiently, which further confirmed the proposed structure shown in Figure 1.

Self-assembly behaviours from ALS

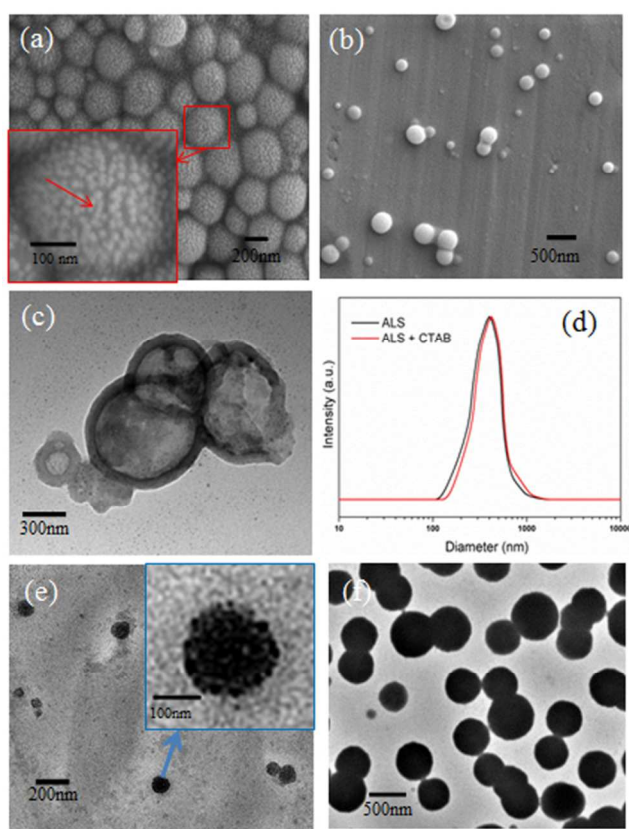


Fig. 4 (a,b) SEM image of nanospheres from ALS alone (ALS aggregates see red arrow); (c) TEM image of ALS hollow nanospheres; (d) DLS of ALS solution of 0.05 mg mL^{-1} in EtOH/H₂O (9/1, v/v); (e,f) TEM image of quasi-solid nanospheres with ALS and CTAB via self-assembly (aggregates see blue box).

ALS, obtained from alky chain coupling polymerization of LS, is an amphiphilic biopolymer due to the presence of hydrophilic groups and its hydrophobic aromatic skeleton. In this work, ALS was used to prepare hollow nanospheres via self-assembly. The ALS was first dissolved in H₂O to prepare 0.50 mg mL^{-1} ALS aqueous solution, followed by the addition of EtOH to achieve the solution of 0.05 mg mL^{-1} . The volume ratio of EtOH/H₂O was 9/1 and the pH of the solution was

around 7.0. We studied the self-assembly carefully with the combination of SEM, TEM, DLS, AFM and XPS.

Figure 4a-b shows a SEM image of the nanospheres obtained from ALS solution. The spherical morphology was clearly demonstrated by scanning electron microscopy. The diameter of the nanospheres was about 100~500 nm. It is known that lignosulfonate exists as nano-size oval-shaped aggregate between 10 and 20 nm in water solution.¹³ More importantly, the nanosphere contained a lot of ALS aggregates as observed by SEM as shown in Figure 4a (red arrows). This result is coincident with the result in previous work¹³ and can be explained with mechanism model in Figure 6. ALS was firstly dissolved in water to achieve 0.50 mg mL^{-1} , which formed a lot of aggregates.¹³ EtOH was added into the ALS aqueous solution and the ALS aggregates began to self-assemble to form smooth nanosphere finally (Figure 4b). Compared to LS, hydrophobic alkyl chain building block in ALS improved the C/S element ratio (see Table 2) and provided higher hydrophobic property, which may contribute to their self-assembly behaviours to obtain nanospheres.^{12,38}

The hollow nature of these nanospheres was evidenced by transmission electron microscopy (TEM), as shown in Figure 4c. The nanospheres exhibited a obvious contrast between the inner part and the peripheral of the spheres, which further supported the hollow nature of the nanospheres detected by SEM above. The diameter of the hollow nanospheres was 100~500 nm, which are very close to the diameter investigated above.

Dynamic light scattering study of the ALS solution can give important information about the solution self-assembly process. As shown in Figure 4d, the average diameter of the nanospheres was about 300 nm, which was in good agreement with the results measured by SEM and TEM. Additionally, particle size distribution of the ALS solution was about 100-700 nm as shown in Figure 4d. It means that nanospheres of different diameters existed in the solution, which may be mainly ascribed to the high polydispersity index (PDI) value of ALS polymer.

ALS aggregates with a lot of sulfonic groups make it tend to assemble with molecules with cationic groups such as CTAB due to the electrostatic interaction between them.³⁹ In this work, ALS polymer were employed for the assembly with CTAB. The preparation was proceeded by adding CTAB dissolved in EtOH to the ALS aqueous solution, and the ratio of n(CTAB): n($-SO_3H$) was 1.5:1. As shown in Figure S1, nanospheres with different diameter from 100 nm to 700 nm were observed by SEM. The structure of the spheres was evidenced by TEM. As shown in Figure 4f, homogeneous quasi-solid nanospheres were obtained by the addition of CTAB molecules. More importantly, the moment of transient that the 100 nm nanosphere contained many solid aggregates ($\sim 15 \text{ nm}$) was also observed by TEM (blue box in Figure 4e) at the same time. The result further confirmed the quasi-solid nature of the sphere. The formation mechanism we proposed in Figure 6 could clearly illustrate the process of self-assembly to obtain quasi-solid spheres. The complexes were formed from ALS and CTAB via electrostatic

interaction, and then the quasi-solid spheres were fabricated from the complexes via self-assembly.

All the above evidence suggested that CTAB molecules with ammonium group promoted the formation of quasi-solid nanospheres via the self-assembly of complexes. It is noteworthy to mention that quasi-solid spheres of different diameters were also observed from 100-500 nm (Figure 4e-f), which was in agreement with the result of DLS shown in Figure 4d. This is mainly ascribed to the high PDI of ultra Mw ALS polymer.

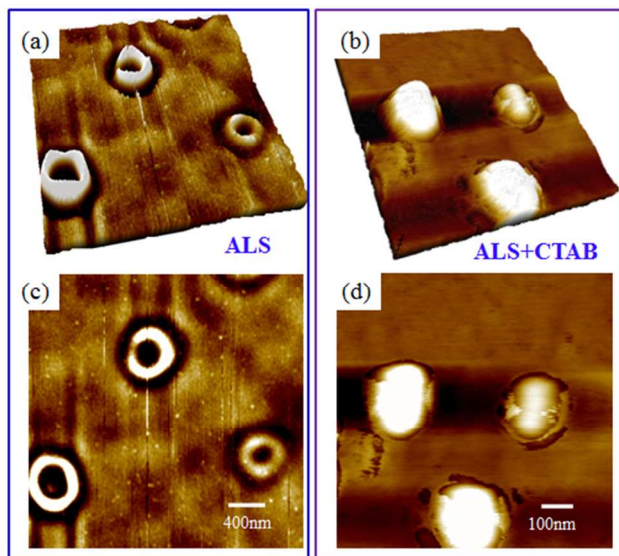


Fig. 5 AFM images of nanospheres after pyrolysis at 800 °C under N₂ atmosphere. (a,c) Hollow nanospheres from ALS alone, (b,d) Quasi-solid nanospheres with ALS and CTAB via self-assembly.

The detailed structure of the hollow sphere and quasi-solid sphere was also investigated using AFM on the morphology of biochar after pyrolysis.⁴⁰ The pyrolysis of both the hollow spheres and quasi-solid spheres were conducted comparatively in a tube furnace under N₂ atmosphere at 800 °C for 2.0 h. As shown in Figure 5, AFM images of hollow spheres and quasi-solid spheres were significantly different. The middle of the hollow sphere was thinner than the periphery, a deep hole was detected after the hollow sphere collapsed in the carbonation process (Figure 5a,c). In contrast, the middle of the quasi-solid sphere obtained from complex of ALS and CTAB was thicker than the periphery, the middle embossment was observed after the quasi-solid sphere collapsed in the carbonation process (Figure 5b,d). The result was in good agreement with the TEM result above, which further confirmed the structure of hollow sphere and quasi-solid sphere.

Table 2 Elemental distribution of LS and ALS bulk materials by elemental analysis method (left), and ALS nanosphere on its surface by XPS (right).

Samples	Elemental analysis			XPS method			
	C%	S%	C/S	C%	S%	C/S	Br%
LS	45.98	5.85	7.86	—	—	—	—
ALS1	53.84	4.18	12.88	71.19	1.84	38.69	—
ALS3	55.03	3.41	16.14	72.14	1.71	42.19	—
ALS5	55.72	3.29	16.94	73.78	1.69	43.66	—

Note: — means none of detection.

That the ALS hollow nanosphere has a hydrophilic core and a hydrophobic shell can be proven by comparing the element ratio of C/S on the nanosphere surface and that of the ALS bulk materials from freeze-drying process. The C/S ratio of ALS was measured by elemental analysis, while the C/S ratio on the surface of hollow nanosphere was estimated by XPS. The results were shown in Table 2 and Figure S2. Hydrophobic association of ALS has higher C/S element ratio comparing with LS, which was a contributing factor on the self-assembly behaviour of ionic polymer.³⁸ Moreover, the C/S element ratio on the surface of ALS hollow nanospheres was obviously higher than those of ALS bulk materials. It gives a direct evident to support that the ALS hollow nanosphere has a hydrophilic core and a hydrophobic shell, which suggested a higher content of -SO₃H groups inside the hollow spheres and more hydrophobic groups on the surface of the hollow spheres.

In addition, X-ray photoelectron spectroscopy (XPS) of ALS spheres was conducted to test the content of bromine element (Figure S2 in SI) and none of Br was detected in all ALSs samples shown in Table 2. If the LS molecules were connected linearly by -C₆H₁₂- groups, under excessive addition of C₆H₁₂Br₂, the -C₆H₁₂Br groups should be detected by XPS. However, none of Br element was detected, which suggested that the mono-substitution reaction of C₆H₁₂Br₂ with LS molecule was negligible and cross-linked network structure of ALSs was proposed to be produced during the polymerization reaction. Thus it further supported the structure of ALS we proposed, as shown in Figure 1. Hence, the general formation mechanism of ALS hollow nanosphere was proposed in Figure 6. ALS aggregates in aqueous solution self-assembly into hollow nanosphere by the addition of EtOH.

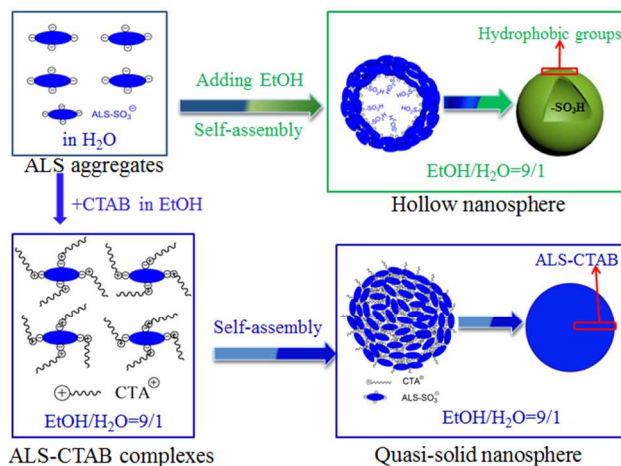


Fig. 6 The proposed formation mechanism of hollow and quasi-solid nanosphere from ALS aggregates.

The elemental distribution of the nanosphere obtained from ALS by addition of CTAB was also detected by elemental analysis and XPS method, as shown in Table S2 and Figure S3. The C/N ratio detected by elemental analysis is very close to that detected by XPS method, which suggested that the homogeneous quasi-solid nanosphere was formed from ALS

and CTAB via self-assembly due to the interaction between sulfonic group of ALS aggregates and amino group of CTAB. In other words, it meant that the C/N ratio on the surface of quasi-solid nanosphere was the same as that of the whole nanosphere. It further supported the results of TEM above that CTAB molecules promoted the self-assembly of ALS aggregate to form quasi-solid nanospheres as shown in Figure 4e.

Furthermore, a content of C (70.51%) on the surface of quasi-solid nanosphere was detected by XPS, higher than that of the whole nanosphere (59.05%) detected by elemental analysis, as shown in Table S2. It illustrated that the hydrophobic chain of some CTAB molecules tended to point away from the quasi-solid sphere. Therefore, the formation mechanism of ALS quasi-solid nanosphere was proposed in Figure 6. The complexes were formed from ALS and CTAB via electrostatic interaction between sulfonic group and amino group, and then the quasi-solid nanosphere was formed by the aggregation of complexes containing ALS and CTAB via self-assembly.

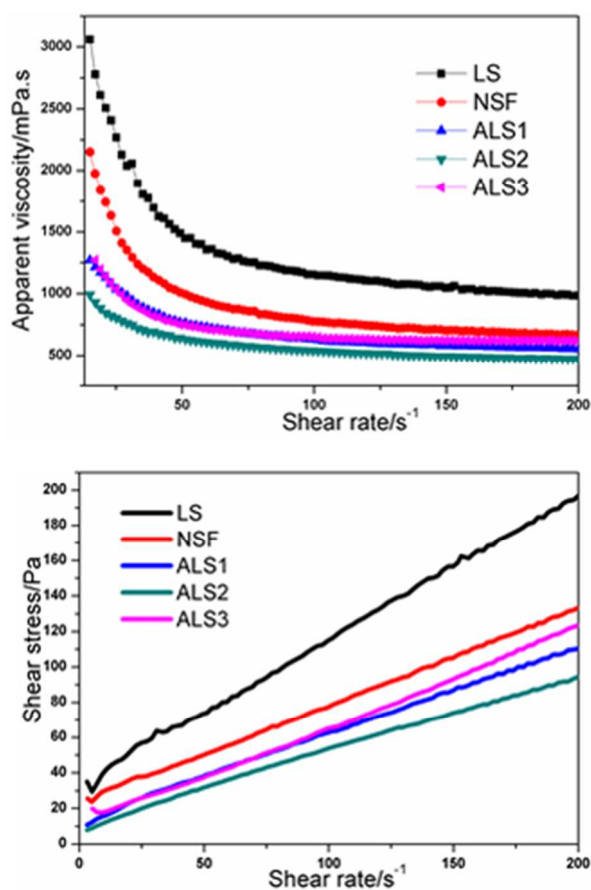


Fig. 7 Apparent viscosity (a) and flow curve (b) of CWSs with Shenhua coal (60.0 wt.% coal content). The dosages of LS, ALSs and NSF for all the CWSs were fixed at 0.6 wt.%.

For coal-water slurry (CWS) applied in industry, low viscosity value and high solid content were expected to insure ease of handling during transfer, storage and atomization.^{21,41} In this study, LS, ALS1, ALS2, ALS3 and NSF were selected to

prepare CWS using Shenhua coal which was a kind of low rank coal (Table S1) and difficult to prepare CWS with a good dispersion property. The dosages of dispersants and the coal contents of each CWS system for all the samples were the same, which were 0.6 wt.% and 60.0 wt.%, respectively. The flow curves of CWS are shown in Figure 7a. Apparent viscosity of CWS using ALSs and NSF as dispersants decreased gradually with increasing of shear rate. The apparent viscosity of CWS with LS was the highest, which meant that the dispersion property of LS was bad. The viscosity values of CWSs with ALSs were lower than NSF, which suggested that ALSs had better effect on reducing the viscosity of the highly concentrated low-rank CWS than that of NSF. ALS2 and NSF were also selected to study the effect of dispersant concentrate on the apparent viscosity of the CWS as shown in Figure S4. The dispersant concentrations varied from 0.3 to 1.4 wt.% (on dry coal basis) and the solid concentration was kept at 60 wt.%. It was revealed from Figure S4 that ALS2 had a better effect on reducing the viscosity of the CWS than that of NSF at different concentrations. The higher molecular weight of lignosulfonate-based dispersant is an important factor influencing its dispersion property.²⁰ The effectiveness of viscosity reduction for CWS with ALS may be also attributed to its cross-linked molecule configuration to have more tight adsorption affinity for coal surface.²¹

Table 3 Fitting rheological parameters calculated by Herschel-Bulkley model of 60 wt.% CWS with different dispersants.

Dispersants	τ_0 (Pa)	K (Pa.S ⁿ)	n	R ²	Apparent viscosity (mPa.s) (at 100 s ⁻¹)
LS	32.03	0.93	0.98	0.9997	1145
NSF	24.07	0.88	1.02	0.9999	773
ALS1	10.51	0.83	0.93	0.9977	625
ALS2	5.79	0.73	0.88	0.9959	536
ALS3	15.45	0.87	0.91	0.9996	639

The application property of coal-water slurry is influenced significantly by the rheological behavior. In this study, the shear stress/shear rate relationship (Figure 7b) was fitted with Herschel-Bulkley fluid obeying equation (1), where τ_0 , K and n denote yield stress, consistency coefficient and flow characteristic exponential, respectively.⁴² The rheological data of the calculated Herschel-Bulkley model parameters were listed in Table 3.

$$\tau = \tau_0 + K\dot{\gamma}^n \quad (1)$$

As shown in Table 3, it suggested that all rheological data represented a good linear relationship as coefficient of correlation (R²) was around 1. The values of flow characteristic exponential (n) for CWS with ALSs were slightly less than 1 which indicated that the slurries belonged to pseudoplastic fluid class. The yield stress τ_0 and consistency coefficient K should be as low as possible for a good dispersant for CWS. As shown in Table 3, ALS2 displayed excellent rheological property because of lower yield stress (5.79 Pa) and lower consistency coefficient (0.73 Pa.Sⁿ), which was good agreement with the result of lower apparent viscosity (536 mPa.s at shear rate of

100 s⁻¹). The results above show that ALSs will be prospective for practical industry application.

Conclusions

A facile method for preparing ALSs with ultrahigh molecular weights, by alkyl chain coupling polymerization using LS as raw materials, has been developed for the first time. GPC, functional group content analyses, FTIR, ¹H-NMR, elemental analyses and XPS further confirmed the cross-linked network structure. The high hydrophobicity of ALS may induce the formation of hollow nanospheres using ALS alone, via self-assembly in selective solvents. In contrast, stable quasi-solid nanospheres were also obtained from ALS and CTAB via self-assembly. ALS2 with moderate molecular weight showed unexpected better dispersion properties than naphthalene sulfonate formaldehyde condensate (NSF) in coal-water slurry. Furthermore, we believe the design concept using LS as raw materials likely can be applied to the synthesis of other lignin and lignosulfonate-based polymers for promising potential industrial applications in future. The successful fabrication of nanomaterials using lignosulfonate-based polymer provide novel avenues for the high value application of abundant bioresource.

Acknowledgements

The authors would like to acknowledge the financial support of National Basic Research Program of China 973 (2012CB215302), International S&T Cooperation Program of China (2013DFA41670), National Natural Science Foundation of China (21436004, 21402054).

Notes and references

^aSchool of Chemistry and Chemical Engineering, South China University of Technology, Guangzhou, China.

Email : celiy@scut.edu.cn, xueqingqiu66@163.com

^bState Key Laboratory of Pulp and Paper Engineering, South China University of Technology, Guangzhou, China.

E-mail: fexwpeng@scut.edu.cn

† Electronic Supplementary Information (ESI) available: Synthetic approach of ALS, The proximate and ultimate analyses for Shenhua coal sample, XPS spectrum of the surface of ALS hollow nanospheres and quasi-solid spheres, SEM and elemental distribution of the quasi-solid nanospheres with ALS and CTAB via self-assembly, Effect of dispersant dosage on the apparent viscosity of CWS with ALSs and NSF. See DOI: 10.1039/x0xx00000x/

- G. A. A. Saracino, D. Cigognini, D. Silva, A. Caprini and F. Gelain. *Chem. Soc. Rev.*, 2013, **42**, 225.
- G. L. Li, H. Mohwald and D. G. Shchukin. *Chem. Soc. Rev.*, 2013, **42**, 3628.
- P. Howes, M. Green, A. Bowers, D. Parker, G. Varma, M. Kallumadil, M. Hughes, A. Warley, A. Brain and R. Botnar. *J. Am. Chem. Soc.*, 2010, **132**, 9833.
- Y. H. Chan, F. M. Ye, M. E. Gallina, X. J. Zhang, Y. H. Jin, I. C. Wu and D. T. Chiu. *J. Am. Chem. Soc.*, 2012, **134**, 7309.
- R. T. Chacko, J. Ventura, J. M. Zhuang and S. Thayumanavan. *Adv. Drug Deliver. Rev.*, 2012, **64**, 836.
- W. S. Choi, J. H. Park, H. Y. Koo, J. Y. Kim, B. K. Cho and D. Y. Kim. *Angew. Chem. Int. Ed.*, 2005, **44**, 1096.
- X. Liu and A. Basu. *J. Am. Chem. Soc.*, 2009, **131**, 5718.
- Y. Y. Mai and A. Eisenberg. *Chem. Soc. Rev.*, 2012, **41**, 5969.
- F. Lu, Y. Luo, B. Li, Q. Zhao and F. J. Schork. *Macromolecules*, 2010, **43**, 568.
- W. Zhou, W. J. Yu and Z. S. An. *Polym. Chem.*, 2013, **4**, 1921.
- S. C. Zimmerman, M. S. Wendland, N. A. Rakow, I. Zharov and K. S. Suslick. *Nature*, 2002, **418**, 399.
- Y. Qian, Y. H. Deng, X. Q. Qiu, H. Li and D. J. Yang. *Green Chem.*, 2014, **16**, 2156.
- X. Q. Qiu, Q. Kong, M. S. Zhou and D. J. Yang. *J. Phys. Chem. B.*, 2010, **114**, 15857.
- R. J. Moon, A. Martini, J. Nairn, J. Simonsen and J. Youngblood. *Chem. Soc. Rev.*, 2011, **40**, 3941.
- Y. B. Huang and Y. Fu. *Green Chem.*, 2013, **15**, 1095.
- J. L. Song, H. L. Fan, J. Ma and B. X. Han. *Green Chem.*, 2013, **15**, 2619.
- T. D. H. Bugg, M. Ahmad, E. M. Hardiman and R. Rahmanpour. *Nat. Prod. Rep.*, 2011, **28**, 1883.
- Y. Sun and J. Y. Cheng. *Bioresource Technol.*, 2002, **83**, 1.
- T. Saito, R. H. Brown, M. A. Hunt, D. L. Pickel, J. M. Pickel, J. M. Messman, F. S. Baker, M. Keller and A. K. Naskar. *Green Chem.*, 2012, **14**, 3295.
- D. J. Yang, X. Q. Qiu, M. S. Zhou and H. M. Lou. *Energ. Convers. Manage.*, 2007, **48**, 2433.
- M. S. Zhou, Q. Kong, B. Pan, X. Q. Qiu, D. J. Yang and H. M. Lou. *Fuel*, 2010, **89**, 716.
- D. J. Yang, X. Q. Qiu, Y. X. Pang and M. S. Zhou. *J. Disper. Sci. Technol.*, 2008, **29**, 1296.
- Z. L. Li, Y. X. Pang, H. M. Lou and X. Q. Qiu. *Bioresources*, 2009, **4**, 589.
- A. Kamoun, A. Jelidi and M. Chaabouni. *Cement Concrete Res.*, 2003, **33**, 995.
- X. J. Wang and J. Zhao. *J. Agr. Food Chem.*, 2013, **61**, 3789.
- Y. Qian, Q. Zhang, X. Q. Qiu and S. P. Zhu. *Green Chem.*, 2014, **16**, 4963.
- M. Tortora, F. Cavaliere, P. Mosesso, F. Ciuffardini, F. Melone and C. Crestini. *Biomacromolecule*, 2014, **15**, 1634.
- M. C. Wang, M. Leitch and C. B. Xu. *Eur. Polym. J.*, 2009, **45**, 3380.
- D. Z. Ye, L. Jiang, C. Ma, M. H. Zhang and X. Zhang. *Int. J. Biol. Macromol.*, 2014, **63**, 43.
- H. M. Lou, H. R. Lai, M. X. Wang, Y. X. Pang, D. J. Yang, X. Q. Qiu, B. Wang and H. B. Zhang. *Ind. Eng. Chem. Res.*, 2013, **52**, 16101.
- H. F. Zhou, D. J. Yang, X. Q. Qiu, X. L. Wu and Y. Li. *Appl. Microbiol. Biotechnol.*, 2013, **97**, 10309.
- H. F. Zhou, J. Y. Zhu, X. L. Luo, S. Y. Leu, X. L. Wu, R. Gleisner, B. S. Dien, R. E. Hector, D. J. Yang, X. Q. Qiu, E. Horn and J. Negron. *Ind. Eng. Chem. Res.*, 2013, **52**, 16057.
- X. P. Ouyang, L. X. Ke, X. Q. Qiu, Y. X. Guo and Y. X. Pang. *J. Dispersion Sci. Technol.*, 2009, **30**, 1.
- A. Tejado, C. Pena, J. Labidi, J. M. Echeverria and I. Mondragon. *Bioresource Technol.*, 2007, **98**, 1655.

Journal Name

- 35 J. Cao, G. Xiao, X. Xu, D. K. Shen and B. S. Jin. *Fuel Process. Technol.*, 2013, **106**, 41.
- 36 B. Joffres, C. Lorentz, M. Vidalie, D. Laurenti, A. A. Quoineaud, N. Charon, A. Daudin, A. Quignard and C. Geantet. *Appl. Catal. B- Environ.*, 2014, **145**, 167.
- 37 A. Toledano, L. Serrano, A. Garcia, I. Mondragon and J. Labidi. *Chem. Eng. J.*, 2010, **157**, 93.
- 38 Y. Li, Y. G. Wang, G. Huang, X. P. Ma, K. J. Zhou and J. M. Gao. *Angew. Chem. Int. Ed.*, 2014, **53**, 9074.
- 39 L. Samokhina, M. Schrinner and M. Ballauff. *Langmuir*, 2007, **23**, 3615.
- 40 X. F. Cao, L. X. Zhong, X. W. Peng, S. N. Sun, S. M. Li, S. J. Liu and R. C. Sun. *Bioresource Technol.*, 2014, **155**, 21.
- 41 G. Atesok, F. Boylu, A. A. Sirkeci and H. Dincer. *Fuel*, 2002, 81, 1855.
- 42 R. Li, D. J. Yang, H. M. Lou, M. S. Zhou and X. Q. Qiu. *Energ. Convers. Manage*, 2012, **64**, 139.